Nanoparticles Complexed with Gene Vectors to Promote Proliferation of Human Vascular Endothelial Cells

*Qian Li, Changcan Shi, Wencheng Zhang, Marc Behl, Andreas Lendlein, and Yakai Feng**

Corresponding Author: Y. Feng, School of Chemical Engineering and Technology, Tianjin University, Tianjin 300072, China

Email: yakaifeng@tju.edu.cn (Y. Feng)

Dr. Q. Li, Dr. C. Shi, Prof. Y. Feng

School of Chemical Engineering and Technology, Tianjin University, Tianjin 300072, China

Prof. W. Zhang

Department of Physiology and Pathophysiology, Logistics University of Chinese People's Armed Police Force, Tianjin 300162, China

Dr. M. Behl, Prof. A. Lendlein, Prof. Y. Feng

Tianjin University-Helmholtz-Zentrum Geesthacht, Joint Laboratory for Biomaterials and Regenerative Medicine, Tianjin 300072, China

Dr. M. Behl, Prof. A. Lendlein

Institute of Biomaterial Science and Berlin-Brandenburg Center for Regenerative Therapies (BCRT), Helmholtz-Zentrum Geesthacht, Kantstr. 55, 14513 Teltow, Germany

Prof. Y. Feng

Key Laboratory of Systems Bioengineering of Ministry of Education, Tianjin University, Tianjin 300072, China

Prof. Y. Feng

Collaborative Innovation Center of Chemical Science and Chemical Engineering (Tianjin),Tianjin 300072, China

ABSTRACT

Amphiphilic block copolymers containing biodegradable hydrophobic segments of depsipeptide based copolymers have been synthesized and explored as gene carriers for enhancing proliferation of endothelial cells *in vitro*. These polymers form nanoparticles (NPs) with positive charges on their surface, which could condense recombinant plasmids of enhanced green fluorescent protein plasmid and ZNF580 gene (pEGFP-ZNF580) and protect them against DNase I. ZNF580 gene is efficiently transported into EA.hy926 cells to promote their proliferation, whereby the transfection efficiency of NPs/pEGFP-ZNF580 is approximately similar to that of Lipofectamine 2000. These results indicate that the NPs might have potential as a carrier for pEGFP-ZNF580, which could support endothelialization of cardiovascular implants.

Keywords: gene carrier, nanoparticles, endothelial cells, proliferation, block copolymer

1. Introduction

Nowadays, many people suffer from cardiovascular disease (CVD). Autologous vein vessels remain the gold standard for microvascular repair as they are both compliant and non-thrombogenic. However, these vessels are not always the best option, because they may be occluded or diseased, especially if the patient already suffers from some sort of peripheral vascular diseases. Thus autologous blood vessels from the patient's own tissue often cannot meet the actual demand for the clinical application of small-diameter blood vessels. While, artificial blood vessels are widely used in clinical applications,[1-3] the application is limited to inside-diameter larger than 6 mm. Small caliber vascular grafts (diameter < 4 mm) are so far associated with an increased risk of thrombosis

and occlusion.[4-6] Therefore, strategies for improving their compliance and hemocompatibility are demanded. One option gaining hemocompatibility is the functionalization of the inner surface with the aim to minimize protein adsorption and to hinder thrombocytes to adhere. For this purpose, hydrophilic surfaces are created by linking, e.g. polyethers or zwitter ionic moieties on the surface of the vascular graft. Examples for improving the hydrophilicity of artificial blood vessels include surface functionalization with poly(ethylene glycol) methacrylate (PEGMA),[7,8] poly(ethylene glycol),[9] 2-methacryloyloxyethyl phosphorylcholine[10-13] or heparin[14,15]. Such surface modifications enhance the hemocompatibility, but at the same time hinder endothelial cells (EC) to attach and cover the graft. Covering the inner surface of an artificial blood vessel with a functional, confluent layer of ECs would mimic healthy blood vessel walls and in this way potentially enable a long term applicability of such implants. The lack of endothelialization on the inner surface of synthetic vessel however results in low patency rate.[16] Different possibilities to specifically enhance adherence, migration and proliferation of ECs on hydrophilic, protein repellent surfaces were explored. Peptides improving EC adherence, e.g. containing Arg-Gly-Asp (RGD) or Arg-Glu-Asp-Val (REDV) sequence were integrated in the surface.[17,18] The release of cytokines promoting the proliferation and migration of ECs was investigated. Another strategy could be based on genetic engineering with ZNF580 gene. The overexpression of ZNF580 in human endothelial cell hybridoma line EA.hy926 cells led to the enhancement of matrix metalloproteinase-2 and vascular endothelial growth factor expression as well as the migration and proliferation of EA.hy926 endothelial cells.[19] These promising *in vitro* results motivate us to explore a genetic engineering strategy with the ZNF580 gene in artificial blood vessels.

Gene therapy is a promising concept for treating diseases. Various types of carriers have been investigated for their capability to deliver therapeutic genes into the desired target cells. An ideal gene

delivery carrier would be a system that can safely transport genes without exhibiting any toxicity and immune responses, and can be synthesized in a large scale.[20,21] Recently, the use of non-viral carriers such as polycationic polymers, polymeric micelles, and nanoparticles to deliver plasmid DNA (pDNA) has been highlighted.[22-24] Polycationic polymers have the ability to physically bind pDNA, and can be applied to a variety of cells. Among the polycationic polymers, polyethylenimine (PEI) has been proven to be an effective transfection agent for the delivery of pDNA into cells both *in vitro* and *in vivo*.[25-27] The high cationic charge density enables PEI to effectively condense pDNA and form nanometric particles, which can be endocytosed.[28-30] The transfection performance of PEI depends on its macromolecular structure and molecular weight. High molecular weight PEI shows high efficiency for gene transfection, but exhibits cytotoxic effects on various cell lines.[31-33] At PEI concentrations used in typical transfection protocols, cell metabolic activity may be reduced by 40-90%.[32,33]

In contrast to high molecular weight PEI, low molecular weight PEI has low cytotoxicity but can not transfer DNA effectively because of the poor DNA condensation capacity.[34] Various methods have been investigated to modify PEI in order to improve its gene transfection efficiency *in vitro*. Thomas and Klibanov [35] reported on hydrophobic modification, i.e., partial dodecylation of the primary amino groups of low molecular weight PEI resulted in efficient and nontoxic carrier. Hydrophilic poly(ethylene glycol) (PEG) or chitosan modified PEI exhibited much lower cytotoxicity and higher transfection efficiency than PEI (25,000 $g \cdot mol^{-1}$).[36-38] Recently, PEI conjugated gold nanoparticles have been used as gene carriers with excellent gene transfection efficiency especially in serum-containing media.[39] In addition, the mesoporous silica nanoparticles have been developed to delivery genes after their surface is functionalized with cationic polymers.[40] Although these inorganic nanoparticles exhibit high gene transfection efficiency and low cytotoxicity *in vitro*, the non-

biodegradability and safety in body are still a serious challenge for *in vivo* application.[41-45] On the other hand, biodegradable polymeric nanocarriers with core-shell structure benefit from biodegradability with the aim to address the non-biodegradability of inorganic nanoparticles. One example is the cationic PEI-poly(ε-caprolactone) polymer as the core-shell nanocarriers.[46,47] The biodegradable polymers can endow gene carriers with nontoxicity, biodegradability as well as a core-shell structure. However there is only limited knowledge whether the chemical modification of low molecular weight PEI with biodegradable polymer segments could lead to efficient gene carriers.

Here we aimed to prepare a gene carrier with low toxicity and the capability to form nanoparticle/gene vector complexes with high transfection efficiency for ECs. A self-assembly process shall be used to prepare core-shell nanoparticles from block copolymers. A biodegradable core consisting of hydrophobic segments shall act as a crosslinking point. Oligomeric PEI (M_w = 1,800 g·mol^{-1}) chains should be preferentially located at the surface of the nanoparticles. Thus these nanoparticles could efficiently condense DNA. We selected hydrophobic copolymers from a depsipeptide and dilactide to covalently link low molecular weight PEIs as depsipeptide based copolymers are biodegradable with beneficial biocompatibility during degradation.[48-52] Our strategy consists of the synthesis of biodegradable block copolymers based on PEI (1,800 g·mol^{-1}) and poly[(L-lactide)-*co*-(3(*S*)-methyl-2,5-morpholinedione)] (P(LA-*co*-MMD)) blocks, and the formation of nanoparticles thereof by self-assembly.[53-55] In our previous study, we have prepared microparticles from mPEG-b-P(MMD-*co*-GA)-g-PEI. The hydrodynamic diameter ranged from 144 to 205 nm because of the long PEG block (M_w = 5000 g·mol^{-1}) formed a thick hydrophilic shell surrounding the core of the microparticle. [53,54] This shell also induced a low zeta potential with values from 19.8±0.7 mV to 24.5±1.0 mV. This hydrophilic shell of PEG can increase the stability of the microparticles, but decreased the transfection efficiency because of the low entrance ability of microparticles into cells. Therefore nanoparticles

with low diameter but high zeta potential should be created for enhancing transfection efficiency. However, polymeric particles usually have the tendency to aggregate and to form larger particles with DNA when the shell has less PEG content as found in our previous study.[56] So we designed and synthesized the degradable polymer P(LA-*co*-MMD) to avoid the aggregation by increasing the core´s stability through the strong hydrogen bond interaction of depsipeptide segments. The core's stability should be increased by the strong interaction, which also favors to form small size particles. We used amphiphilic block copolymers PEI-P(LA-*co*-MMD) in order to prepare the nanoparticles in this paper, because they had high PEI content but did not have PEG block. The block copolymers were investigated for their physicochemical properties with gel permeation chromatography (GPC), Fourier transform infraredspectroscopy (FT-IR), nuclear magnetic resonance (NMR), and dynamic light scattering, for their *in vitro* release function, and finally for their biofunctionalities such as cytotoxicity, resistance to nuclease degradation and gene transfection ability.

2. Materials and Methods

2.1 Materials

Polyethylenimine (branched PEI, M_w = 1,800 $g \cdot mol^{-1}$) and stannous octoate ($Sn(Oct)_2$) were purchased from Sigma-Aldrich (St. Louis, USA). LA was obtained from Foryou Medical Device Co., Ltd. (Huizhou, China). 1,8-Octanediol was purchased from Heowns Biochem Technologies Co., Ltd. (Tianjin, China). Isophorone diisocyanate (IPDI) was supplied from Hersbit Chemical Co., Ltd. (Shanghai, China). 3-(4,5-Dimethyl-2-thiazolyl)-2,5-diphenyl-2-H-tetrazolium bromide (MTT) was purchased from DingGuo ChangSheng Biotech. Co., Ltd. (Beijing, China). Dimethyl sulphoxide (DMSO) was purchased from Sigma (St. Louis, MO). Lipofectamine 2000 reagent was purchased from Invitrogen (Grand Island, USA). BCA protein assay kit was purchased from Solarbio Science

and Technology Co., Ltd. (Beijing, China). Rabbit anti-human ZNF580 polyclonal antibody and goat anti-rabbit IgG were purchased from Abcam (HK) Ltd. (Hongkong, China). The pEGFP-ZNF580 was preserved by Department of Physiology and Pathophysiology, Logistics University of Chinese People's Armed Police Force. 3(*S*)-Methyl-2,5-morpholinedione (MMD) was prepared according to reported method.[57]

2.2 Synthesis of Amphiphilic Block Copolymers

2.2.1 Synthesis of P(LA-co-MMD)

P(LA-*co*-MMD) copolymers were prepared as reported previously by ring-opening polymerization (ROP).[58] Three copolymers named P(LA-*co*-MMD)$_1$, P(LA-*co*-MMD)$_2$ and P(LA-*co*-MMD)$_3$ were obtained, in which the subscripts 1, 2 and 3 indicate the MMD contents (10 wt%, 20 wt% and 30 wt%) in feed (Supporting Table S1).

2.2.2 Synthesis of Amphiphilic Block Copolymers

P(LA-*co*-MMD) (1.0 g) was dissolved in chloroform (9.5 mL), then the solution was transferred into a dried constant pressure funnel. Dibutyltin dilaurate (DBTDL, 10 μL) and IPDI (10 wt% toluene solution, 769 μL) were added in a three-necked flask, the above P(LA-*c*o-MMD) solution was added dropwise during stirring at 30 °C for 30 min, and reacted for 12 h. The reaction mixture was precipitated in dry n-hexane (100 mL), dried under at room temperature under vacuum for 24 h until constant weight was achieved.

The α,ω-diisocyanto P(LA-*co*-MMD) (0.40 g, 0.035 mmol) was dissolved in 5.0 mL chloroform, and added dropwise into 15 wt% PEI toluene solution (PEI 0.63 g, 0.35 mmol) under a nitrogen atmosphere at 60 °C for 12 h. The resultant copolymer was cooled to room temperature and then precipitated in excess cold petroleum ether. Here, PEI-P(LA-*co*-MMD)$_1$, PEI-P(LA-*co*-MMD)$_2$, PEI-P(LA-*co*-MMD)$_3$ were prepared from P(LA-*co*-MMD)$_1$, P(LA-*co*-MMD)$_2$, P(LA-*co*-MMD)$_3$,

respectively.

2.3 Characterization of the Copolymers

FT-IR spectra of the copolymers were obtained using a FT-IR spectrometer (Bio-Rad FTS-6000, USA). Moreover, ^{1}H-NMR spectra of the synthesized polymers were recorded with a Bruker Avance spectrometer (AV-400, Bruker, Karlsruhe, Germany) operating at 400 MHz in DMSO-d_6. The weight average molecular weight (M_w) was determined by gel permeation chromatography (GPC) using four Waters Styragel columns (HT 2, HT 3, HT 4, and HT 5), a Waters 1515 isocratic HPLC pump, and a Waters 2414 RI detector. Tetrahydrofuran (THF) was used as the eluent at a flow rate of 1.0 mL/min. Polystyrene standards were used for the calibration.

2.4 Degradation of P(LA-co-MMD)$_2$ Copolymer

The copolymers were dissolved in THF solvent and casted into films. Once completely dried, the films were cut into small pieces with dimensions of 10 × 10 × 0.2 mm^3 and put in a screw vial containing 80 mL PBS (pH = 7.4). The vials were put in the constant temperature air bath shaker (50 rpm) and incubated at 37 °C for 35 days. The PBS buffer was changed every 5 days. The samples were removed at various time points, and rinsed repeatedly with ultrapure water, and then placed in a vacuum oven. The samples were dried to constant weight at room temperature. The residual weight (%) was calculated using the following formula.

$$\text{Residual weight (\%)} = \frac{W_t}{W_0} \times 100\% \qquad (1)$$

W_0 was the initial weight of the sample, W_t was the weight of sample at different time points.

2.5 Preparation of Nanoparticles

Briefly, PEI-P(LA-*co*-MMD) (10.0 mg) was dissolved in THF (1 mL) and afterwards this solution was slowly added to double distilled water (10 mL). The mixture solution was stirred at room temperature to remove THF, and the final volume was adjusted to 10 mL for further experiments.

2.6 Preparation of NPs/DNA of Complexes

pEGFP-ZNF580 plasmid was diluted to 1 μg/50 μL with PBS buffer. The complexes were prepared by adding NP suspension to plasmid solution (containing 1 μg pDNA) at various N/P molar ratios (N/P molar ratios were calculated from weight of block polymers and pDNA, where N is the content of the polymer and P the content of plasmid) by pipetting and were afterwards incubated for 30 min before characterization and gene transfection experiments.

2.7 Characterization of Particle Size and Zeta Potential

The size and zeta potential of NPs and NPs/pEGFP-ZNF580 complexes were measured using a Zeta sizer 3000HS (Malvern Instrument, Inc., Worcestershire, UK) at the wavelength of 677 nm with a constant angle of 90°.

2.8 Agarose Gel Electrophoresis

To assess DNA condensation ability of the NPs, agarose gel electrophoresis was carried out. The NPs/pEGFP-ZNF580 complexes with different N/P molar ratios ranging from 1 to 30 were prepared as described above. NPs/DNA complexes suspension (10 μL) was mixed with 6x loading buffer (2 μL) and loaded into a 0.8 wt% agarose gel containing 0.5 $\mu g \cdot mL^{-1}$ ethidium bromide. Electrophoresis was set up in 1x TAE buffer at 120 V and kept for 30 min. DNA retardation was analyzed on UV illuminator to indicate the location of the DNA.

2.9 *In vitro* Release Studies

The profiles of *in vitro* pEGFP-ZNF580 release from NPs were measured over 28 days with a method analogous to the procedure reported in Ref. [59]. Briefly, the NPs/pEGFP-ZNF580 complexes with various N/P molar ratios ranging from 10 to 30, containing pEGFP-ZNF580 (20 μg) in each Eppendorf tube, were incubated in Tris-HCl buffer (200 μL) (pH = 7.4) in a shaking incubator at 37 °C. At different time intervals, the complexes solution was centrifuged at 12,000 rpm, 4 °C for 20

min; the supernatant was taken out carefully. Then, the complexes were resuspended with fresh Tris-HCl buffer and reincubated. The adsorption efficiency of pDNA was determined by measuring the extinction fluorescence with ethidium bromide, the supernatant was analyzed using Cary Eclipse fluorescence spectrometer at excitation wavelength of 524 nm and emission wavelength of 582 nm.

2.10 Exposure of the Nanoparticles to DNase I

DNase I mediated digestion was evaluated using agarose gel electrophoresis to evaluate whether PEI-P(LA-*co*-MMD) nanoparticles can protect adsorbed DNA from nucleases digestion.[60,61]

2.11 Cytotoxicity/Cell Viability Studies

EA.hy926 cells (1×10^4 cell/well) were seeded in 96-well plate, and cultured for 24 h until 80-90% confluence. Then, the medium was replaced with serum-free medium. After 12 h, the medium was changed versus fresh growth medium (10 wt% fetal bovine serum (FBS) Dul becco`s modified Eagle´s medium (DMEM)). NP suspension of different concentration and various N/P molar ratios of NPs/pEGFP-ZNF580 complexes were added into the medium. After 48 h, the supernatant was discarded, 20 μL MTT solution (5 $mg{\cdot}mL^{-1}$) was added to each well and formazan crystals were allowed to form for another 4 h. Then, the medium was removed carefully, dimethyl sulfoxide (150 μL) was added to each well, the plate was oscillated at low speed on the volatility instrument for 10 min. Optical density (OD) was measured by an ELISA reader (Titertek multiscan MC) at the wavelength of 490 nm. The relative cell viability (%) was calculated using the following equation. Here, OD490' is the absorbance value of experimental wells minus zero wells, and avg(OD490C') is the average absorbance value of control wells.

$$\text{Relative cell viability (\%)} = \frac{\text{OD490}'}{\text{avg}(\text{OD490C}')} \times 100 \qquad (2)$$

2.12 *In vitro* Transfection Experiments

EA.hy926 cells were seeded in 24-well plate at a density of 1×10^4 cell/well and cultured for 24 h until

80-90% confluence. Before transfection, cells were incubated with serum-free medium for 12 h. NPs/pEGFP-ZNF580 complexes with a N/P molar ratio of 10 (1 μg pEGFP-ZNF580 per well) were added into wells. After 4 h the medium was changed with fresh growth medium (10 wt% FBS DMEM). Then, cells were incubated, the expression of green fluorescence protein (GFP) in cells was observed under an inverted fluorescent microscope at 12 and 48-hour time points.

2.13 *In vitro* Scratch Assay

A scratch wound healing assay was used to evaluate the migration capability of EA.hy926 cells transfected by NPs/pEGFP-ZNF580 complexes. In brief, EA.hy926 cells were transfected with NPs/pEGFP-ZNF580 complexes at the N/P molar ratio of 10; 48 h later, the transfected cells were incubated to produce a nearly confluent cell monolayer in a 6-well plate. A liner wound was subsequently generated in the monolayer using a sterile 200 μL plastic pipette tip. Cellular debris was removed by washing with D-hanks buffer (pH = 7.4). The migration process at different time points was monitored by capturing images using an inverted microscope; the migration area was calculated using Image J 2.1 based on the images after 12 h. The percentage of migration area was calculated by the following equation.

$$\text{Migration area } (\%) = \frac{\text{wounded area} - \text{nonrecovered area}}{\text{wounded area}} \times 100 \qquad (3)$$

2.14 Western Blot

Western blot analysis was performed as reported previously.[62]

2.15 Statistical Analysis

Quantitative data are expressed as means ± standard deviation. Statistical analysis was performed by single-factor analysis of variance. p values less than 0.05 were considered to be statistically significant.

3 Results

3.1 Synthesis and Characterization of PEI-P(LA-*co*-MMD) Block Copolymers

PEI-P(LA-*co*-MMD) copolymers were synthesized according to **Scheme 1**. The P(LA-*co*-MMD) copolymers were synthesized from MMD and LA by ROP with 1,8-octanediol as an initiator. MMD was copolymerized with LA to form copolymers with a random sequence structure. The weight average molecular weight (M_w) of these copolymers was determined by GPC (see in Supporting Table S1). M_w of P(LA-*co*-MMD) copolymers ranged from 10,800 $g{\cdot}mol^{-1}$ to 11,000 $g{\cdot}mol^{-1}$ with polydispersity index (PDI) value of 1.42 – 1.52. The contents of MMD in copolymers were calculated from ^{1}H-NMR, and found to be slightly lower than in the feed ratio (Supporting Table S1). PEI-P(LA-*co*-MMD) block copolymers had M_w with the range from 14,900 $g{\cdot}mol^{-1}$ to 15,500 $g{\cdot}mol^{-1}$ with PDI of 1.56 – 1.62 (Supporting Table S2).

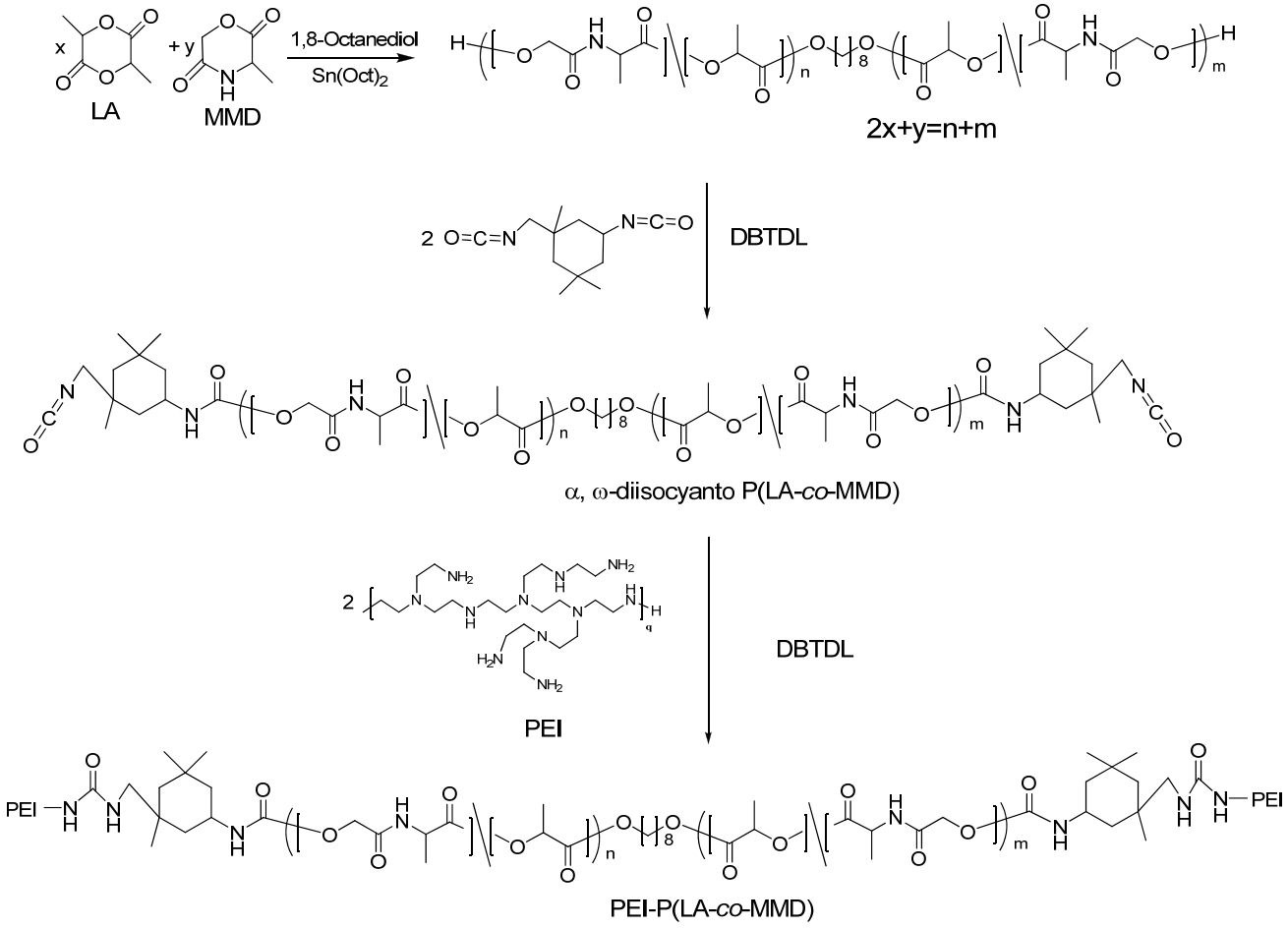

Scheme 1. Synthesis route of amphiphilic block copolymers from biodegradable depsipeptide based copolymers and PEI.

As shown in Supporting Figure S1, P(LA-*co*-MMD) copolymers presented a strong signal at 1749 cm^{-1}, which was assigned to the carbonyl groups in LA and MMD segments. The peak at 1694 cm^{-1} was attributed to the secondary amide in MMD segments. The stretching frequency at 1085 cm^{-1} indicated the ester group (-O-C=O). The broad absorption band at 3378 cm^{-1} was assigned to the stretch of -NH- group in MMD. These results indicated a successful integration of MMD units into the copolymer. The characteristic peaks can be observed clearly in FT-IR spectrum of the block copolymer PEI-P(LA-*co*-MMD). The absorption intensity at 3378 cm^{-1} increased owing to PEI and MMD. The symmetric stretching vibration peaks appearred at 3378 cm^{-1} and 1659 cm^{-1} owing to the primary amine in PEI, and the stretching frequency at 1538 cm^{-1} representive the -NH- in PEI.

^{1}H-NMR spectra of the copolymers measured at room temperature are shown in **Figure 1**. The peaks corresponding to MMD and LA could be clearly observed in the spectra and assigned as follow: 5.15 ppm (O=C-C**H**-O, 1H, LA segment), 1.63 ppm (O-CH-C**H$_3$**, 3H), 4.8-4.9 ppm (O=C-C**H$_2$**-O, 2H, MMD segment), 4.42 ppm (NH-C**H**-CH$_3$, 1H), 1.56 ppm (NH-CH-C**H$_3$**, 3H), 8.5 ppm (CH-N**H**, 1H), 2.4-3.2 ppm (-NH-C**H$_2$**-C**H$_2$**-, PEI segment). These results suggest the successful synthesis of the PEI-P(LA-*co*-MMD) block copolymers.

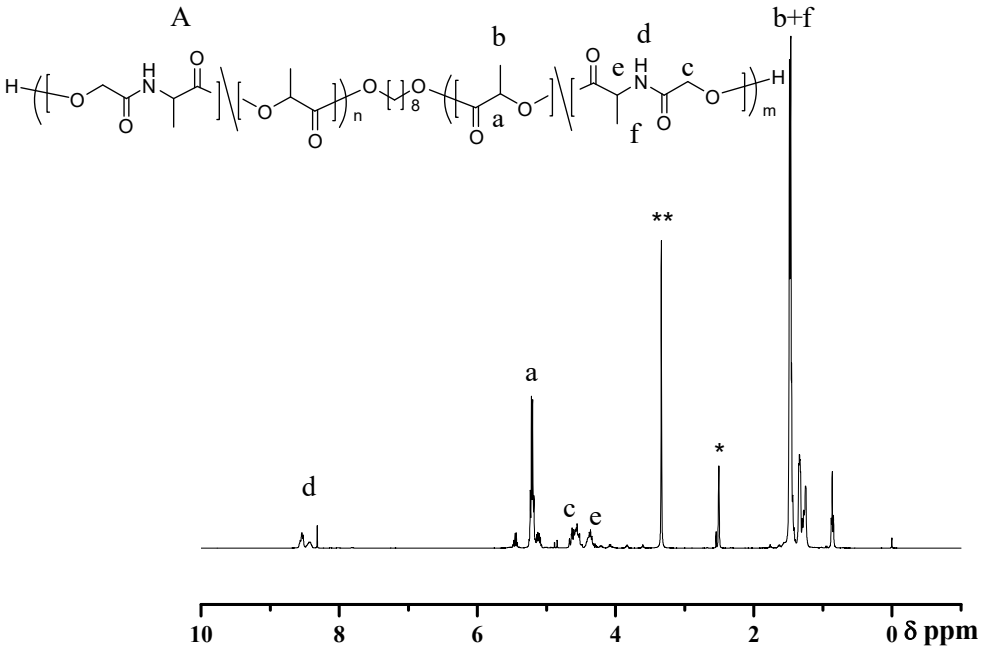

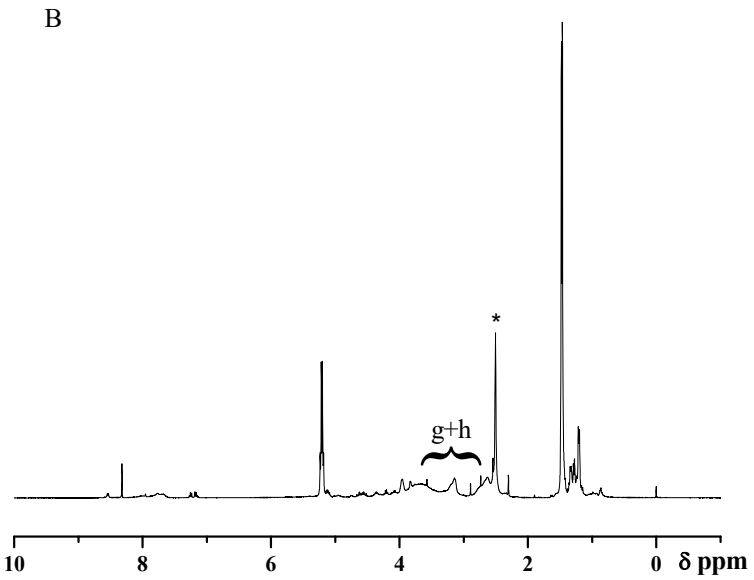

Figure 1. ^{1}H-NMR spectra of (A) P(LA-*co*-MMD)$_2$, (B) PEI-P(LA-*co*-MMD) block copolymer using DMSO-d$_6$ as solvent and TMS as internal reference, *Solvent peak. **H_2O.

3.2 Characterization of Nanoparticles

3.2.1 Particle size and zeta potential of PEI-P(LA-co-MMD) nanoparticles

As an amphiphilic copolymer, PEI-P(LA-*co*-MMD) can self-assemble into nanoscaled particles. The hydrodynamic diameter and zeta potential of NPs were measured with a nanoparticle size and zeta potential analyzer, the obtained values of mean size and zeta potential are summarized in **Table 1**. The results indicated that the size of NPs ranged between 95.2 nm and 160.3 nm with a reasonable polydispersity index from 0.22 to 0.40. The zeta potential of NPs ranged between 28.0 mV and 36.2 mV. The high potential of NPs is beneficial to the stability of nanoparticles in the suspension. The phenomenon such as coalescence and precipitation did not occur when NPs suspension was kept for

a long time. In the following study, PEI-P(LA-*co*-MMD)$_2$ based NPs were selected as an example because of their small size (95.2±6.1 nm) and high zeta potential (28.0±1.1 mV).

Table 1 Nanoparticle size, polydispersity index and zeta potential of PEI-P(LA-*co*-MMD) and NPs/pEGFP-ZNF580 complexes at different N/P molar ratios

Sample ID	Size (nm)	*PDI*[a)]	Zeta Potential (mv)
PEI-P(LA-*co*-MMD)$_1$	134.2±6.6	0.35	31.2±0.9
PEI-P(LA-*co*-MMD)$_2$	95.2±6.1	0.22	28.0±1.1
PEI-P(LA-*co*-MMD)$_3$	160.3±14.9	0.40	36.2±1.6
N/P 10[b)]	80.8±4.4	0.23	3.4±0.7
N/P 20[b)]	78.4±5.2	0.33	7.3±0.6
N/P 30[b)]	74.7±4.9	0.28	11.5±0.9

[a)]*PDI*: Polydispersity index

[b)]PEI-P(LA-*co*-MMD)$_2$ NPs/pEGFP-ZNF580 complexes at N/P molar ratios of 10, 20, and 30. Amphiphilic block copolymers have been synthesized and explored as gene carriers to promote the proliferation of endothelial cells in vitro. NPs/pEGFP-ZNF580 complexes might enhance endothelialization of artifi cial blood vessels.

3.2.2 Degradation of P(LA-co-MMD)$_2$ copolymer

The hydrolytic degradation of the P(LA-*co*-MMD)$_2$ copolymers as the hydrophobic core was investigated. Poly(L-lactide) (PLA) was used as control group. *In vitro* degradation experiments at 37 °C in aqueous phosphate buffer solution (PBS) with a pH of 7.4 revealed a higher hydrolytic degradation rate of P(LA-co-MMD)$_2$ copolymer compared to PLA as shown in Supporting Figure S2. The high degradation rate was attributed to the depsipeptide unit in P(LA-*co*-MMD)$_2$ chains. Depsipeptide unites provide amide and ester groups, which improve the hydrophilicity of the copolymer. During degradation, water diffused easily into materials. Moreover, the existence of

depsipeptide unites in P(LA-*co*-MMD)$_2$ copolymer chains hindered the crystallization. The block copolymers with lower crystalline degree degraded faster than PLA (Supporting Table S1).[63]

3.2.3 Morphology of NPs and NPs/pEGFP-ZNF580 complexes

As shown in **Scheme 2**, amphiphilic block copolymers can assemble into core-shell structure NPs in aqueous solution. P(LA-*co*-MMD) hydrophobic segments of the amphiphilic block copolymer formed the core of NPs, while the hydrophilic PEI segments could form the cationic shell and hydrophilic corona.

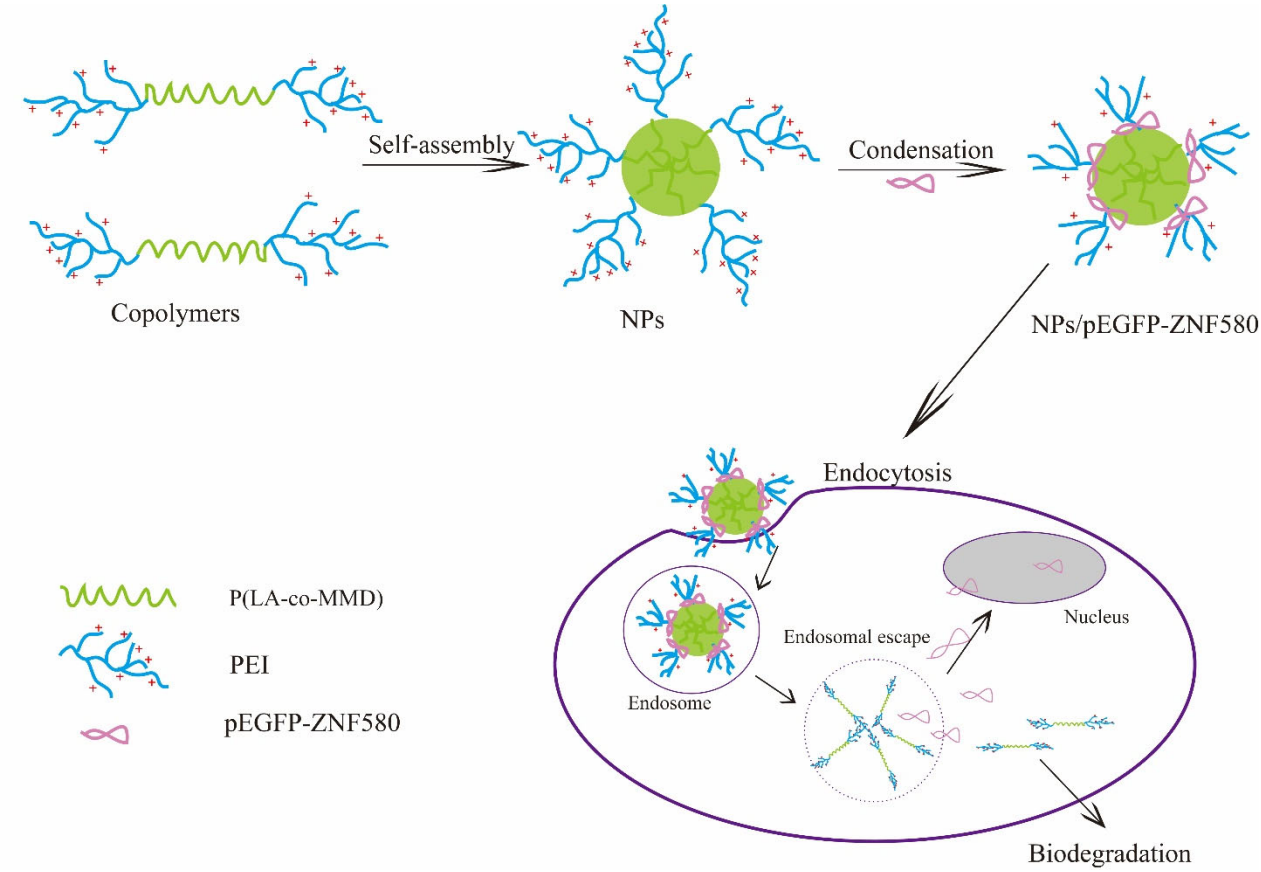

Scheme 2. Formation of nanoparticles from PEI-P(LA-*co*-MMD) block copolymers and process of delivery of pEGFP-ZNF580 into EA.hy926.

The suitable size and net charge of NPs/pEGFP-ZNF580 complexes are two significant factors for

polycations used as gene carriers to be internalized into cells.[64,65] Table 1 shows the mean size and zeta potential values of NPs/pEGFP-ZNF580 complexes, which are measured at different N/P molar ratios. The sizes of NPs/pEGFP-ZNF580 complexes at the N/P molar ratios of 10, 20, and 30 were 80.8±4.4 nm, 78.4±5.2 nm and 74.7±4.9 nm, which declined a little compared with NPs. This could be explained by the fact that the formation of complexes with pEGFP-ZNF580 is through ionic interactions.[53, 66]

The nano-size of these NPs/pEGFP-ZNF580 makes them suitable for uptake by cells, which is the first step for gene delivery.[67] Zeta potential of these NPs/pEGFP-ZNF580 complexes increased from 3.4 mV to 11.5 mV with the increasing of N/P molar ratio from 10 to 30. The suitable net positive charge on the surface can facilitate adherence to negatively charged cellular membranes, inducing and increasing intracellular uptake.[68]

3.3 Agarose Gel Electrophoresis of NPs/pEGFP-ZNF580 Nanocomplexes

The effective condensation of negatively charged DNA into nanoparticles through electrostatic interactions is important for well-designed gene carriers.[69] Agarose gel electrophoresis was performed to investigate the condensation capability of NPs to DNA for the binding efficiency qualitatively and quantitatively.

NPs/pEGFP-ZNF580 complexes with different N/P molar ratios were incubated at room temperature for 30 min before gel retardation assay. The images are shown in **Figure 2**a. It was observed that pEGFP-ZNF580 could migrate to the positive electrode under the electric field. Once pEGFP-ZNF580 was associated with the NPs which was too large to diffuse through the agarose matrix, the mobility of pEGFP-ZNF580 was hindered and it was detained in the well of the agarose gel. The results indicated that when the mass ratio of NPs to pEGFP-ZNF580 reached 10 or above, pEGFP-

ZNF580 was combined with NPs. In the following study, high N/P molar ratio (≥ 10) was selected due to the perfect binding effect.

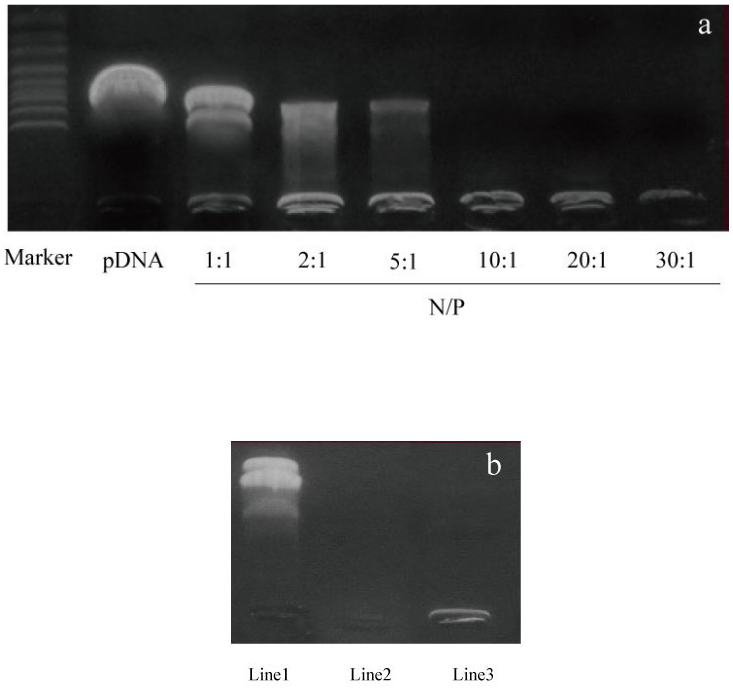

Figure 2. Agarose gel electrophoresis of NPs/pEGFP-ZNF580 complexes at various N/P molar ratios. pDNA is pEGFP-ZNF580. (a) N/P molar ratios were 1:1, 2:1, 5:1, 10:1, 20:1, and 30:1. (b) Agarose gel electrophoresis for assessment of plasmid stabilization against DNase I degradation after the incubation for 30 min. Line 1: non-treated pDNA as control, Line 2: pDNA after incubation with DNase I at 0.1 U/μg pDNA, Line 3: NPs/pEGFP-ZNF580 complex at the N/P molar ratio of 10 after incubation with DNase1 at 0.1 U/μg pDNA.

3.4 *In vitro* Release Studies

The sequential release of plasmid is one of the important functions for gene carriers in gene therapy. **Figure 3** shows the accumulative release (expressed as percentage of loaded pEGFP-ZNF580) of pEGFP-ZNF580 from NPs/pEGFP-ZNF580 complexes *in vitro* during 28 days. An initial increase in release of pEGFP-ZNF580 was observed for NPs/pEGFP-ZNF580 complexes in the first week, which can be attributed to a fast penetration of water into the hydrophilic PEI segments and their

removal by diffusion within the first 7 days. After 7 days, 44.5% of pEGFP-ZNF580 was released from NPs/pEGFP-ZNF580 complexes at the N/P molar ratio of 10. Its initial and overall release was found to be statistically higher than that at the N/P molar ratio of 20 and 30 ($p < 0.05$). Because the electrostatic interaction between NPs and pEGFP-ZNF580 increased when the N/P molar ratio increased. The release of DNA could be maintained nearly one month, furthermore, the release speed of pEGFP-ZNF580 decreased with the increase of the N/P molar ratio. However, Lipofectamine 2000/pEGFP-ZNF580 showed a rapid release. Compared with Lipofectamine 2000/pEGFP-ZNF580, all the NPs/pEGFP-ZNF580 at different N/P molar ratios have sequential release ($p < 0.05$). These results showed that the release of pEGFP-ZNF580 can be controlled by this kind of gene carriers.

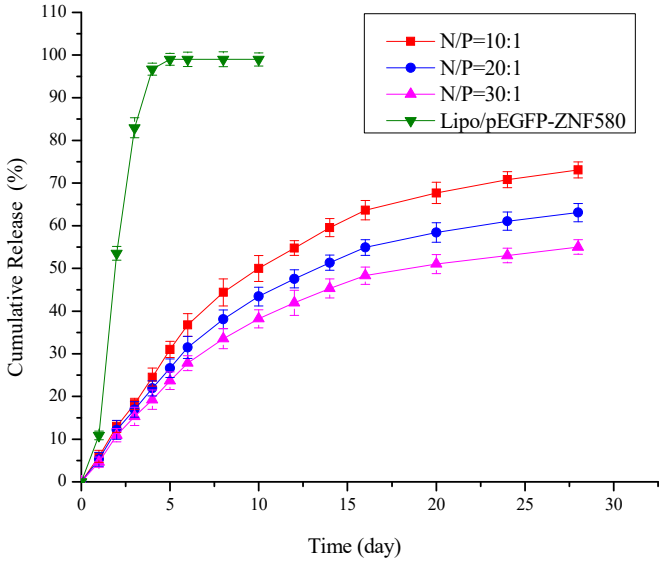

Figure 3. Cumulative release of pEGFP-ZNF580 from NPs/pEGFP-ZNF580 and Lipofectamine 2000/pEGFP-ZNF580 complexes at different N/P molar ratios.

3.5 Protection Effect from DNase I Degradation

The protection of pDNA from nucleases is essential for efficient gene delivery *in vitro* and *in vivo*.[70]

We investigated whether the NPs/pEGFP-ZNF580 complexes could protect the loaded pEGFP-ZNF580 from DNase I *in vitro*. As shown in Figure 2b, the pEGFP-ZNF580 was completely digested by DNase I at 0.1 $U \cdot \mu g^{-1}$ DNA within 30 min of incubation. In contrast, NPs/pEGFP-ZNF580 complexes could protect the loaded pEGFP-ZNF580 from degradation by DNase I.

3.6 Cytotoxicity Evaluation of NPs and NPs/pEGFP-ZNF580

The cytotoxicity of NPs and NPs/pEGFP-ZNF580 was evaluated *in vitro* by MTT assay. The cytotoxicity of PEI-P(LA-*co*-MMD)$_2$ blank NPs and NPs/pEGFP-ZNF580 complexes at various concentrations against EA.hy926 cell is shown in **Figure 4**. PEI (M_w = 1800 $g \cdot mol^{-1}$) and PEI/pEGFP-ZNF580 complexes were used as control groups. The EA.hy926 cell viability decreased with the increased concentration of NPs and NPs/pEGFP-ZNF580 (**Figure 4**). At the same concentration, the cell viabilities of NPs and NPs/pEGFP-ZNF580 were significantly higher than that of PEI (M_w = 1800 $g \cdot mol^{-1}$) and PEI/pEGFP-ZNF580 complexes as the control groups ($p < 0.05$). Compared with NPs, NPs/pEGFP-ZNF580 complexes showed a relatively low cytotoxic effect. Cell viability was higher than 80% even at a concentration of 100 $\mu g \cdot mL^{-1}$ NPs/pEGFP-ZNF580 complexes. At a low concentration (less than 40 $\mu g \cdot mL^{-1}$), NPs/pEGFP-ZNF580 complexes not only exhibited non-cytotoxicity, but also promoted the proliferation of cells. This is owing to low molecular weight PEI (M_w = 1,800 $g \cdot mol^{-1}$) having low cytotoxicity. Moreover, the positive charge of NPs could be counterbalanced by the negative charge of pEGFP-ZNF580 to minimize the direct contact with the cell membrane.[71] The results indicated that this kind of NPs/pEGFP-ZNF580 complexes could be a suitable non-cytotoxic gene carrier to be used in our future experiments. Considering the cell viabilities of NPs/pEGFP-ZNF580 complexes, the concentration of 40 $\mu g \cdot mL^{-1}$ was used in the following experiments.

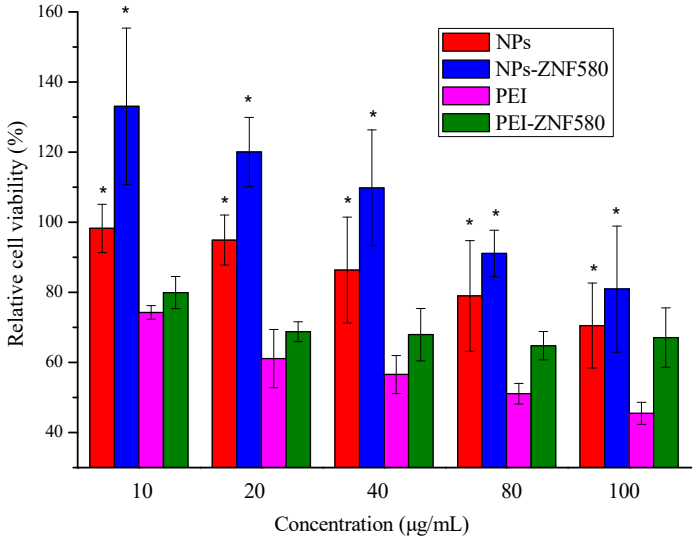

Figure 4. Relative cell viability of EA.hy926 cells after 48 h of treatment with varying concentrations of NPs and NPs/pEGFP-ZNF580 complexes at N/P molar ratio of 10 (x+SD, n = 6, *p < 0.05 *vs.* PEI group), PEI (M_w = 1800 g·mol^{-1}) and PEI/pEGFP-ZNF580 complexes as control groups.

3.7 *In vitro* Transfection Studies

In an *in vitro* transfection study the ability of NPs/pEGFP-ZNF580 complexes with a N/P molar ratio of 10 and the concentration of 40 μg·mL^{-1} to transfer pEGFP-ZNF580 into EA.hy926 cells was determined. Cells transfected with pEGFP-ZNF580 by Lipofectamine 2000 and PEI (M_w = 1800 g·mol^{-1}) were used as the positive controls in our study. Lipofectamine 2000 is well known to provide high transfection efficiency and high level of transgene expression *in vitro.* Cells treated with pDNA served as negative control. The transfected EA.hy926 cells showed green fluorescence (**Figure 5**a). But the pDNA could barely transfect EA.hy926 cells in the negative control group. After 48 hours, the transfection efficiency of NPs/pEGFP-ZNF580 was approximately similar to that of Lipofectamine 2000. Compared with PEI/pEGFP-ZNF580 group, NPs/pEGFP-ZNF580 group

showed obviously high transfection efficiency. The quantification data for transfection efficiency were shown in **Figure 5**b. The results indicate a successful transfection and expression of EA.hy926 cells by pEGFP-ZNF580.

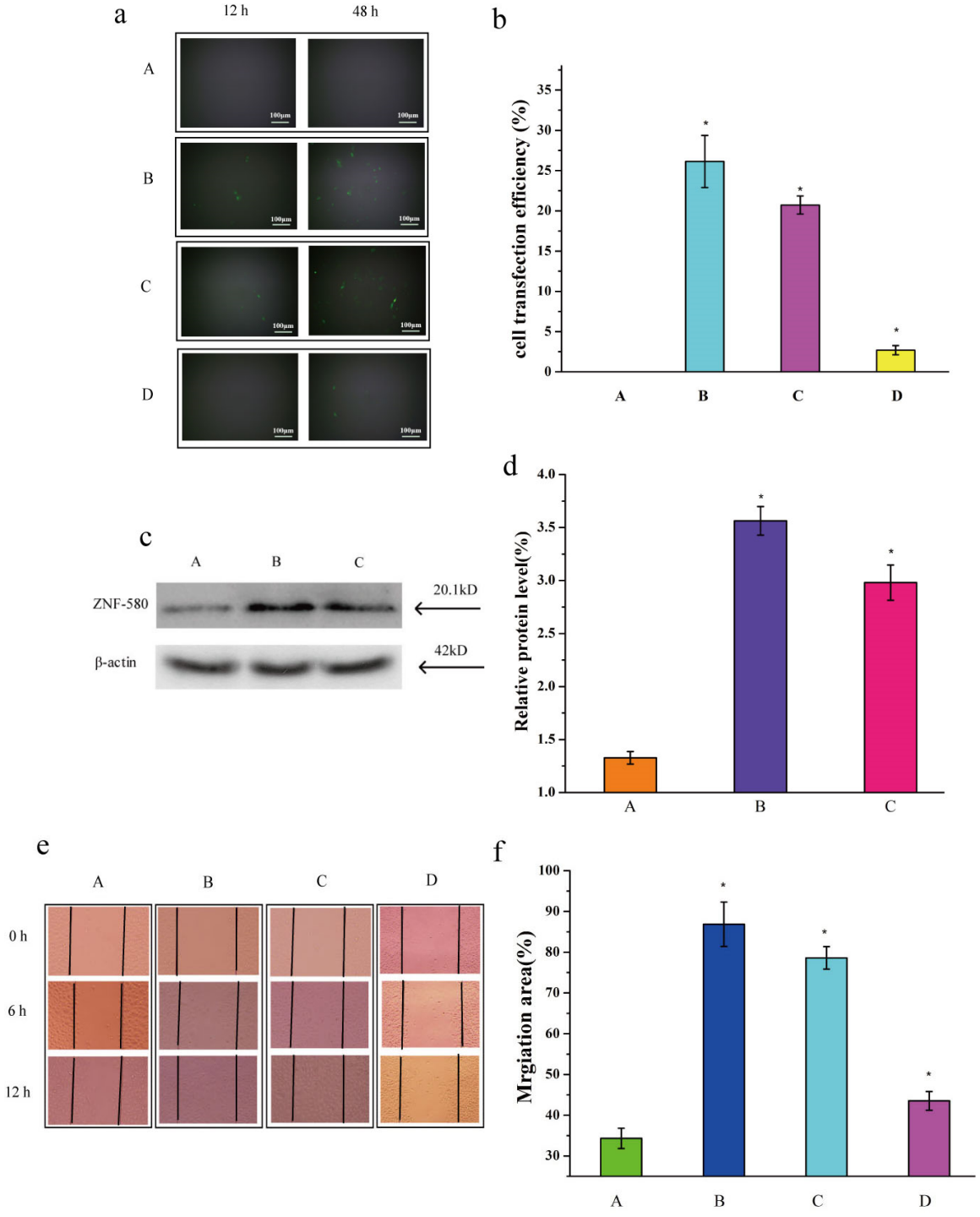

Figure 5. Proliferation of EA.hy926 cells mediated by NPs/pEGFP-ZNF580 complexes at the concentration of 40 $\mu g \cdot mL^{-1}$. (a) Fluorescence images of EA.hy926 cells transfected by NPs/pEGFP-ZNF580 complexes with a N/P molar ratio of 10 at time intervals of 12 h and 48 h. The Lipofectamine 2000 group is the positive control group, pDNA group served as the negative control group. (b) Cell transfection efficiency (%) after 48h was evaluated in transfected cells compared with control group cells. (c) Western blot analysis for ZNF580 protein expression in EA.hy926 cells transfected by NPs/pEGFP-ZNF580 complexes and Lipofectamine 2000 after 48 h. (d) ZNF580 relative protein level (%) was evaluated by the expression of pEGFP-ZNF580 in transfected cells compared with control group cells ($p < 0.05$). (e) Migration process of EA.hy926 cells at 0, 6, and 12 h. (f) Migration area (%) after 12 h calculated by Image-Pro Plus (6.0) (A) EA.hy926 treated with pDNA as the control group, (B) Cells transfected by NPs/pEGFP-ZNF580 complexes (N/P molar ratio = 10), (C) Cells transfected by Lipofectamine 2000 (x+SD, n = 3, *$p < 0.05$ *vs.* control group). (D) Cells transfected with PEI/pEGFP-ZNF580 complexes (M_w = 1800 $g \cdot mol^{-1}$) (x+SD, n = 3, *$p < 0.05$ *vs.* control group).

3.8 Western blot

Western blot analysis was performed to explore the level of ZNF-580 protein expression. NPs/pEGFP-ZNF580 complexes and Lipofectamine 2000 were used to transfect the EA.hy926 cells. ZNF580 relative protein level (%) was evaluated by the expression of pEGFP-ZNF580 in transfected cells compared with control group cells ($p < 0.05$). As shown in **Figure 5c**, ZNF580 was detected in the cytosolic fraction as a 20.1 kDa band whereas β-actin was detected as a 42 kDa band. When the ZNF580 expression value of the control group was compared to NPs/pEGFP-ZNF580, a significant increase was observed in **Figure 5d**. In addition, the transfection efficiency of NPs/pEGFP-ZNF580 complexes was little higher than that of Lipofectamine 2000. These results demonstrate that ZNF580

plasmids can be released from the NPs/pEGFP-ZNF580 complexes and expressed successfully in EA.hy926 cells.

3.9 *In vitro* Scratch Assay

Figure 5e showed the *in vitro* scratch assay to assess the migration ability of cells. EA.hy926 cells were transfected with NPs/pEGFP-ZNF580 complexes at the N/P molar ratio of 10 and the concentration of 40 $\mu g \cdot mL^{-1}$. EA.hy926 cells treated with Lipofectamine 2000 and PEI (M_w = 1800 $g \cdot mol^{-1}$) were used as positive controls and treated with pDNA were used as a negative control. After 48 h, a liner wound was subsequently generated. The images showed that the cells transfected with NPs/pEGFP-ZNF580, Lipofectamine 2000 and PEI/pEGFP-ZNF580 migrated at a fast rate compared with the negative control cells in the same dish. Furthermore, cells that were transfected with NPs/pEGFP-ZNF580 complexes showed a migration rate of about 86.8±5.5%, which was nearly 8% higher than Lipofectamine 2000 and nearly 43% higher than PEI/pEGFP-ZNF580 (**Figure 5f**). The result indicated that EA.hy926 cells transfected with NPs/pEGFP-ZNF580 complexes showed a wonderful prospect to promote their migration and proliferation.

4. Discussion

Gene delivery technology is explored for enhancing the endothelialization on the inner surface of artificial blood vessels. In this paper, we report about a biodegradable gene carrier with low toxicity. Amphiphilic block copolymers PEI-P(LA-*co*-MMD) were synthesized from MMD, LA, and low molecular weight PEI in a two-step synthesis route. Firstly, biodegradable depsipeptide based copolymers P(LA-*co*-MMD) were synthesized from MMD and LA by ROP. And then, PEI-P(LA-*co*-MMD) block copolymers were obtained by covalently linking PEI to P(LA-co-MMD) with

diisocyanates as junction units.

Depsipeptides based copolymers contain repeating units with amide and ester groups.[72] They degrade partly to produce L-amino acids that buffer the pH of the degradation microenvironment, which reduces the inflammation caused by the acidic environment generated during the degradation of aliphatic polyesters such as PLA. The P(LA-*co*-MMD) copolymers exhibit a higher hydrolytic degradation rate than homopolymer PLA, because high hydrophilicity is favored for water diffusion into materials. The core of a single nanoparticle contains P(LA-*co*-MMD) segments, whereas hydrophilic short PEI chains were preferentially located on the surface of NPs. These short PEI chains formed the out shell of the NPs with zeta-potential of 28.0 mV - 36.2 mV, thus the NPs could condense DNA and deliver plasmids into cells efficiently.

The positive surface charge of PEI was one of the properties required to interact with the pDNA.[73] The imine groups of the PEI in PEI-P(LA-*co*-MMD) were bound with the phosphate groups of pEGFP-ZNF580 by electrostatic interaction. Besides, particle size apparently affected the transfection efficiency of gene carriers.[74] Large particles were poorly internalized by the cells, so the desirable carriers should be small to have effective endocytosis.[75] In this respect, the prepared NPs with a high zeta-potential (> 28.0 mV) and small particle size (less than 160 nm) could condense pDNA to form NPs/pEGFP-ZNF580 complexes. The zeta-potential of the NPs/pEGFP-ZNF580 complexes decreased to 3.4 mV - 11.5 mV, and particle size also decreased to 74.7 nm - 80.8 nm.

The N/P molar ratio depended on the condensation, especially zeta-potential and particle size of the NPs/pEGFP-ZNF580 complexes. The prepared gene carriers completely condensed the pEGFP-ZNF580 onto its surface to form NPs/pEGFP-ZNF580 complexes when the N/P molar ratio was 10 or above 10. Furthermore, the NPs can protect pEGFP-ZNF580 against DNase I at this N/P molar ratio. This means that many short PEI chains could efficiently condense pDNA into the out shell of

the NPs and deliver the gene into cells.

The cytotoxicity of a polymeric gene carrier is an important factor affecting transfection efficiency. The cell viability was more than 70% even when the concentration of blank NPs was 100 $\mu g \cdot mL^{-1}$. For NPs/pEGFP-ZNF580 complexes, even lower cytotoxicity was found. The NPs degraded into lower molecular segment leading to low cytotoxicity because the low molecular weight PEI has low cytotoxicity.

In vitro transfection studies, ZNF580 gene promoted the proliferation and migration of ECs. The transfection effect of NPs/pEGFP-ZNF580 complexes was approximately similar to that of Lipofectamine 2000. Our results demonstrated that pEGFP-ZNF580 was carried into ECs through these gene carriers at appropriate N/P. This is owing to positive charged PEI-shell (low molecule weight PEI) of NPs. The western blot result indicated that the expression of ZNF580 key protein increased to 3.5%. The migration rate of ECs transfected by NPs/pEGFP-ZNF580 was promoted significantly (migration area 86.8±5.5% in 12 h). By this way, NPs/pEGFP-ZNF580 was suitable for transfection and could be used as a potential delivery system to promote the proliferation of endothelial cells. In the future, we will use these NPs/pEGFP-ZNF580 complexes to enhance the rapid endothelialization of artificial blood vessels in order to cover the inner surface with a functional layer of ECs. This should potentially enable a long term application of such implants.

5. Conclusions

PEI-P(LA-*co*-MMD) nanoparticles were prepared successfully and evaluated for their gene carrier capacity by transferring pEGFP-ZNF580 gene into ECs. This NPs/pEGFP-ZNF580 complex had low cytotoxicity and enhanced the proliferation and migration ability of ECs. Therefore, the amphiphilic block copolymers have the potential as safe and efficient gene carriers, and the NPs/pEGFP-ZNF580

complexes might enhance the rapid endothelialization of artificial blood vessels.

Supporting Information

Supporting Information is available from the Wiley Online Library or from the author.

Acknowledgements

This project was supported by the National Natural Science Foundation of China (Grant No. 31370969), the International Cooperation from Ministry of Science and Technology of China (Grant No. 2013DFG52040), Ph.D. Programs Foundation of Ministry of Education of China (No. 20120032110073) and the Program of Introducing Talents of Discipline to Universities of China (No. B06006).

References

[1]. B. H. Walpoth, G. L.Bowlin, *Expert Rev. Med. Dev.* 2005, *2*, 647.

[2]. O. E. Teebken, A. Haverich, *Eur. J. Vasc. Endovasc. Surg.* 2002, *23*, 475.

[3]. E. D. Boland, J. A. Matthews, K. J. Pawlowski, D. G. Simpson, G. E. Wnek, G. L. Bowlin, *Front. Biosci.* 2004, *9*, 1422.

[4]. D. S. Baim, *J. Am. Coll. Cardiol.* 2003, *42*, 1370.

[5]. H. Wang, Y. Feng, Z. Fang, W. Yuan, M. Khan, *Mater. Sci. Eng. C* 2012, *32*, 2306.

[6]. R. Virchow, *Nutr. Rev.* 1989, *47*, 23.

[7]. W. Yuan, Y. Feng, H. Wang, D. Yang, B. An, W. Zhang, M. Khan, J. Guo, *Mater. Sci. Eng. C* 2013, *33*, 3644.

[8]. H. Zhao, Y. Feng, J. Guo, *J. Appl. Polym. Sci.* 2011, *119*, 3717.

[9]. R. R. Janairo, Y. Zhu, T. Chen, S. Li, *Tissue Eng. Part A.* 2014, *20(1-2)*, 285.

[10]. Y. Feng, D. Yang, M. Behl, A. Lendlein, H. Zhao, J. Guo, *Macromol. Symp.* 2011, *309*, 6.

[11]. W. Gao, Y. Feng, J. Lu, M. Khan, J. Guo, *Macromol. Res.* 2012, *20*, 1063.

[12]. B. Gao, Y. Feng, J. Lu, L. Zhang, M. Zhao, C. Shi, M. Khan, J. Guo, *Mater. Sci. Eng. C* 2013, *33*, 2871.

[13]. Y. Liu, Y. Inoue, A. Mahara, S. Kakinoki, T. Yamaoka, K. Ishihara, *J. Biomater. Sci. Polym. Ed.* DOI: 10.1080/09205063.2014.920172

[14]. M. Tan, Y. Feng, H. Wan, L. Zhang, M. Khan, J. Guo, Q. Chen, J. Liu, *Macromol. Res.* 2013, *21*, 541.

[15]. F. P. Seib, M. Herklotz, K. A. Burke, M. F. Maitz, C. Werner, D. L. Kaplan, *Biomaterials* 2014 *35*, 83.

[16]. J. Yu, A. Wang, Z. Tang, J. Henry, B. L. P. Lee, Y. Zhu, F. Yuan, F. Huang, S. Li, *Biomaterials* 2012, *33*, 8062.

[17]. Z. Zhang, Y. Lai, L. Yu, J. Ding, *Biomaterials* 2010, *31*, 7873.

[18]. Y. Wei, Y. Ji, L. Xiao, Q. Lin, J. Xu, K. Ren, J. Ji, *Biomaterials* 2013, *34*, 2588.

[19]. H. Sun, S. Wei, R. Xu, P. Xu, W. Zhang, *Biochem. Biophys. Res. Commun.* 2010, *395*, 361.

[20]. S. Jin, K. Ye, *Biotechnol. Prog*. 2007, *23*, 32.

[21]. S. H. Ku, K. Kim, K. Choi, S. H. Kim, I. C. Kwon, *Adv. Healthcare Mater.* 2014, *3*, 1182.

[22]. Y. Kakizawa, K. Kataoka, *Adv. Drug Deliv. Rev.* 2002, *54*, 203.

[23]. C. Shi, F. Yao, J. Huang, Q. Li, M. Khan, Y. Feng, W. Zhang, *Biomaterials* 2014, *35*, 7133.

[24]. S. Rhaese, H. von Briesen, H. R.Waigmann, J. Kreuter, K. Langer, *J. Control. Release* 2003, *92*, 199.

[25]. J. Choi, J. Choi, H. Suh, J. Park, *Bull. Korean Chem. Soc.* 2001, *22*, 46.

[26]. D. Fischer, T. Bieber, Y. Li, H. P. Elsasser, T. Kissel, *Pharm. Res.* 1999, *16*, 1273.

[27]. M. Neu, D. Fischer, T. Kissel, *J. Gene Med.* 2005, *7*, 992.

[28]. A. Harpe, H. Petersen, Y. Li, T. Kissel, *J. Control. Release* 2000, *69*, 309.

[29]. R. Kircheis, L. Wightman, E. Wagner, *Adv. Drug Deliv. Rev.* 2001, *53*, 341.

[30]. C. Yang, W. Cheng, P. Y. Teo, A. C. Engler, D. J. Coady, J. L. Hedrick, Y. Y. Yang, *Adv. Healthcare Mater.* 2013, *2*, 1304.

[31]. G. Cheng, Y. He, L. Xie, Y. Nie, B. He, Z. Zhang, Z. Gu, *Int. J. Nanomedicine.* 2012, *7*, 3991.

[32]. Y. Lim, S. Kim, H. Suh, J. Park, *Bioconjugate Chem.* 2002, *13*, 952.

[33]. M. L. Forrest, J. T. Koerber, D. W. Pack, *Bioconjugate Chem*. 2003, *14*, 934.

[34]. H. Petersen, K. Kunath, A. L. Martin, S. Stolnik, C. J. Roberts, M. C. Davies, T. Kissel, *Biomacromolecules* 2002, *3*, 926.

[35]. M. Thomas, A. M. Klibanov, *Proc. Natl. Acad. Sci. U.S.A.* 2002, *99*, 14640.

[36]. Z. Zhang, C. Yang, Y. Duan, Y. Wang, J. Liu, L. Wang, D. Kong, *Acta Biomater.* 2010, *6*, 2650.

[37]. Z. Zhong, F. Jan, M. C. Lok, W. E. Hennink, L. V. Christensen, J. W. Yockman, Y. H. Kim, S. W. Kim, *Biomacromolecules* 2005, *6*, 3440.

[38]. K. Wong, G. Sun, X. Zhang, H. Dai, Y. Liu, C. He, K. W. Leong, *Bioconjugate Chem.* 2006, *17*, 152.

[39]. H. Tian, Z. Guo, J. Chen, L. Lin, J. Xia, X. Dong, X. Chen, *Adv. Healthcare Mater.* 2012, *1*, 337.

[40]. M. Khan, Z. Y. Ong, N. Wiradharma, A. B. E. Attia, Y. Yang, *Adv. Healthcare Mater.* 2012, *1*, 373.

[41]. S. Sharma, S. Chockalingam, P Sanpui, A. Chattopadhyay, S. S. Ghosh, *Adv. Healthcare Mater.* 2014, *3*, 106.

[42]. E. Locatelli, F. Broggi, J. Ponti, P. Marmorato, F. Franchini, S. Lena, and M. C. Franchini, *Adv. Healthcare Mater.* 2012, *1*, 342.

[43]. X. Ma, X. Wang, M. Zhou, H. Fei, *Adv. Healthcare Mater.* 2013, *2*, 1038.

[44]. N. R. Panyala, E. M. Peña-Méndez, J. Havel, *J. Appl. Biomed.* 2009, *7*, 75.

[45]. B. Fadeel, A. E. Garcia-Bennett, *Adv. Drug Delivery Rev.* 2010, *62*, 362.

[46]. T. K. Endres, M. B. Broichsitter, O. Samsonova, T. Renette, T. H. Kissel, *Biomaterials*, 2011, *32*, 7721.

[47]. M. Zheng, Y. Liu, O. Samsonova, T. Endres, O. Merkel, T. Kissel, Int. J. Pharm. 2012, *427*, 80.

[48]. Y. Feng, M. Behl, S. Kelch, A. Lendlein, *Macromol. Biosci.* 2009, *9*, 45.

[49]. Y. Feng, J. Guo, *Int. J. Mol. Sci.* 2009, *10*, 589.

[50]. Y. Feng, J. Lu, M. Behl, A. Lendlein, *Int. J. Artif. Organs* 2011, *34*, 103.

[51]. A. Battig, B. Hiebl, Y. Feng, A. Lendlein, M. Behl, *Clin. Hemorheol. Microcirc.* 2011, *48*, 161.

[52]. L. Zhang, Y. Feng, J. Lv, J. Yang, H. Tian, C. Shi, M. Zhao, J. Guo, *React. Funct. Polym.* 2013, *73*, 1281.

[53]. C. Shi, F. Yao, J. Huang, G. Han, Q. Li, M. Khan, Y. Feng, W. Zhang, *J. Mater. Chem. B* 2014, *2*, 1825.

[54]. S. Shi, M. Fan, X. Wang, C. Zhao, Y. Wang, F. Luo, X. Zhao, Z. Qian, *J. Phys. Chem. C* 2010, *114*, 21315.

[55]. M. Elfinger, C. Pfeifer, S. Uezguen, M. M. Golas, B. Sander, C. Maucksch, H. Stark, M. K. Aneja, C. Rudolph, *Biomacromolecules* 2009, *10*, 2912.

[56]. J. Lv, X. Hao, J. Yang, Y. Feng, M. Behl, A. Lendlein, *Macromol. Chem. Phys.* DOI: 10.1002/macp.201400345.

[57]. Y. Feng, C. Chen, L. Zhang, H. Tian, W. Yuan, *Trans. Tianjin Univ.* 2012, *18*, 315.

[58]. Q. Guo, T. Liu, X. Yan, X. Wang, S. Shi, F. Luo, Z. Qian, *Int. J. Nanomed.* 2011, *6*, 1641.

[59]. M. Gargouri, A. Sapin, B. A. Yegin, J. L. Merlin, P. Becuwe, P. Maincent, *Int. J. Pharm.* 2011,

403, 276.

[60]. S. Vimal, G. Taju, K.S.N. Nambi, S. Abdul Majeed, V. Sarath Babu, M. Ravi, A.S. Sahul Hameed, *Aquaculture* 2012, *358-359*, 14.

[61]. C. L. Gebhart, S. Sriadibhatla, S. Vinogradov, P. Lemieux, V. Alakhov, A. V. Kabanov, *Bioconjugate Chem.* 2002, *13*, 937.

[62]. D. Ren, H. Wang, J. Liu, M. Zhang, W. Zhang, *Mol. Cell Biochem.* 2012, *359*, 183.

[63]. Y. Feng, J. Lu, M. Behl, A. Lendlein, *Macromol. Biosci.* 2010, *10*, 1008.

[64]. X. Xu, H. Yuan, J. Chang, B. He, Z. Gu, *Angew. Chem. Int. Ed.* 2012, *51*, 3130.

[65]. S. Guo, Y. Huang, T. Wei, W. Zhang, W. Wang, D. Lin, X. Zhang, A. Kumar, Q. Du, J. Xing, L. Deng, Z. Liang, P. C. Wang, A. Dong, X. Liang, *Biomaterials* 2011, *32*, 879.

[66]. H. Lu, Y. Dai, L. Lv, H. Zhao, *PLoS ONE* 2014, *9(1)*: e84703.

[67]. R. Arote, T. H. Kim, Y. K. Kim, S. K. Hwang, H. L Jiang, H. H. Song, J. W. Nah, M. H. Cho, C. S. Cho, *Biomaterials* 2007, *28*, 735.

[68]. M. B. Benita, S. Romeijn, H. E. Junginger, G. Borchard, *Biopharm.* 2004, *58*, 1.

[69]. Q. F. Zhang, W. J. Yi, B. Wang, J. Zhang, L. Ren, Q. M. Chen, L. Guo, X. Q. Yu, *Biomaterials* 2013, *34*, 5391.

[70]. W. Zou, C. Liu, Z. Chen, N. Zhang, *Int. J. Pharm.* 2009, *370*, 187

[71]. K. Kunath, A. Harpe, D. Fischer, H. Petersen, U. Bickel, K. Voigt, T. Kissel, *J. Control. Release* 2003, *89*, 113.

[72]. J. Lv, L. Zhang, M. Khan, X. Ren, J. Guo, Y. Feng, *React. Funct. Polym.* 2014, *82*, 89-97.

[73]. I. S. Kim, S. K. Lee, Y. M. Park, Y. B. Lee, S. C. Shin, K. C. Lee, I. J. Oh, *Int. J. Pharm.* 2005, *298*, 255.

[74]. D. M. Xu, S. D. Yao, Y. B. Liu, K. L. Sheng, J. Hong, P. J. Gong, L. Dong, *Int. J. Pharm.* 2007,

338, 291.

[75]. M. R. Park, K. O. Han, I. K. Han, M. H. Cho, J. W. Nah, Y. J. Choi, C. S. Cho, *J. Control. Release* 2005, *105*, 367.